J. Condensed Matter Nucl. Sci. 15 (2015) 92–101

Research Article

Incremental High Energy Emission from a ZrO_2–PdD Nanostructured Quantum Electronic Component CF/LANR

Mitchell Swartz*

JET Energy, Inc., Wellesley Hills, MA 0248, USA

Abstract

In situ measurement for possible incremental penetrating ionizing radiation output from an activated nanocomposite ZrO_2–PdD CF/LANR component revealed a barely detectable, incremental emission when there was significant energy gain. The autonomous driver minimized background radiobiological interference. This effort demonstrates that CF/LANR is relatively safe, with penetrating ionizing emissions, at these power levels, of lower biological impact than typical background sources.
 ISSN 2227-3123

Keywords: High energy CF/LANR emission, Preloaded CF/LANR component, quantum electronic cold fusion component, ZrO_2–PdD CF/LANR nanostructure

1. Background

1.1. Introduction

Lattice assisted nuclear reactions (LANR) use hydrogen-loaded alloys to create heat and other reactions with an energy density 'off the chart' [1,2]. They are an energy multiplier because the energy density of LANR reactions is ten million times that of gasoline. In the case of LANR, there can rarely occur, in a lattice under special conditions, the fusion of two heavy hydrogen nuclei to form a helium nucleus at near room temperature. LANR will play a critical role in many future technologies with potential revolutionary applications to all energy issues – robotics, transportation, electricity production, artificial internal organs, and space travel [1]. So for quality assurance it is important to ascertain the safety of these systems (Fig. 1) in order to evaluate risk/benefit and possible shielding and occupancy issues.

*E-mail: mica@theworld.com

 ISSN 2227-3123

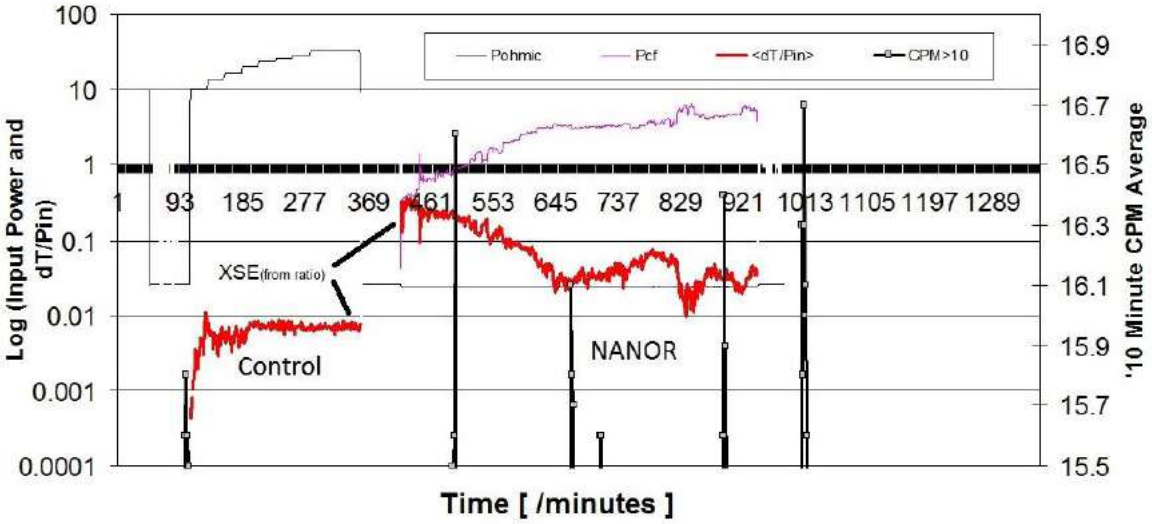

Figure 1. Input power, calorimetry, and gamma measurements of background, thermal control and a CF/LANR system – Shown are the Input Power in milliwatts and Resulting delta-Temperature normalized to the electrical input power (presented as the logarithm on the left hand y-axis), and the 10 min averaged output from the CPM (right hand y-axis) Geiger Müller tube (СИ29БГ tube and TTL serial converter), which was vicinal to a self-contained CF/LANR quantum electronic component containing active preloaded ZrO_2–PdD nanostructured material at its core. The curves are shown as a function of time in minutes ("Counts"). The activity (excess power gain) of the active CF/LANR system is obtained from the ratio of dT/P_{in}(NANOR) to dT/P_{in}(Control)).

1.2. Penetrating radiation and particle emissions

Although LANR is a nuclear process, gamma emission is actually forbidden, both in CF/LANR and in hot fusion as well. For hot fusion, the forbidden restriction is "lifted" by the high temperature, and so penetrating gamma emission is really observed. However at lower temperature, the equations indicated a decrease of forward directed penetrating radiation [3,4] which is observed, and so for cold fusion, (excess) heat and ^{4}He are the usual products, and only rarely have charged particles, gamma radiation, and neutrons also been detected [1]. Diligent efforts with autoradiography and CR-39 have heralded the recording of rare, high energy penetrating radiation emitted from cold fusion (LANR) materials in their active state; in the past usually confirmed by autoradiography or CR-39 chips over periods of days. Miles (China Lake, USN) and M. Srinivasan (Bhabha Atomic Research Center (BARC)) independently used dental X-ray film autoradiography on the outside of the cells which revealed fogging heralding low energy X-ray production [5,6]. M. Srinivasan (BARC) reported neutrons in 1989 as the current increased beyond 100 amperes, neutron signals, in bursts, resulted in 6 of 11 cells [7]. Thereafter, energetic charged particles were detected by CR-39 in gas LANR systems [8] and in aqueous codeposition systems [8]. X.Z. Li (Tsinghua U) first used CR-39 in his 1990 Pd gas loading experiments to detect energetic charged particles [9]. Forsley and Mosier-Boss (SPAWAR) reported CR-39 tracks which indicate possible neutron interactions, including carbon shattering. Some tracks herald D-D and DT reactions. Etching suggests uniformity in the 2–8 MeV range. The triple tracks, found in ∼5–10% of their experiments, indicate energetic neutrons having shattered a carbon atom. Also observed in LANR systems are post LANR mini-explosions, ionizing radiation, and neutron production, and tritium production. These observations of significant quantities of high energy charged particles, and emissions, in LANR systems, suggests that, although very few investigators have looked

with adequate equipment, there is accumulating, near overwhelming, evidence that nuclear reactions in, and assisted by a lattice, are initiated at low energies.

2. Experimental

2.1. Problems

The first problem with quantitation of possible emissions by a detector (Geiger Müller tube, for example) is that very low numbers of neutrons and charged particles appear to be emitted. The second problem is that such penetrating ionizing radiation emissions might be similar to the near infrared (NT-NIR) emissions [10] from active LANR materials which only occur when the CF/LANR devices are active near their optimal operating point (OOP) [11,12]. Third, the output from CF/LANR devices are very low level and can be interfered with by environmental contamination. People with ^{40}K and uranium and thorium in their bodies each contribute ∼0.4 mSv/year. Cosmic rays, radon progeny and terrestrial sources each contribute 0.3, 0.2, and 0.6 per year. Therefore, the only source which could interfere (and irregularly interfere) was removed. A pretested NANOR®-type system was therefore used at a number of input powers [13,14], and it was run autonomously over several weeks.

2.2. Materials

LANR (CF) activated nanocomposite ZrO_2–PdNiD and ZrO_2–PdD CF/LANR quantum electronic components are capable of significant energy gain [13,2]. They are produced in codeposition structures [15] and have been observed producing non-thermal near infrared emissions when active [10], and exhibiting LANR excess heat correlated with the size of the Pd–D nanostructures [15]. Nanostructured materials used in LANR include palladium black [16] in a double structure (DS)-cathode, and today, second and third generation nanostructured ZrO_2–PdD and ZrO_2–PdNiD powders, such as Zr 67% Ni 29% Pd 4% (by weight before the oxidation step). For NANOR®-type LANR devices, the fuel for the nanostructured material resides, ready in the core, and is deuterium (Fig. 2).

The component used here is self-contained, two-terminal NANOR®-type LANR device that features new composition, structure, and superior handling properties enabling portability and transportability. It contains active ZrO_2–PdD nanostructured material loaded with additional D. The deuterons are tightly packed (“highly loaded”). The additional D yields apparent indicated loadings (ratio to Pd) of more than 130% D/Pd, but shallow traps are not ruled out. For simplicity, all of these nanostructured materials in the core, in their range of deuterations, will henceforth simply be

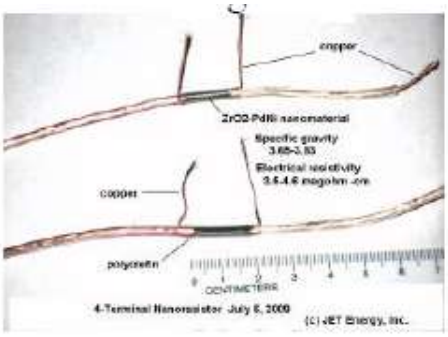

Figure 2. The source of the GM irradiation were NANOR CF/LANR devices. Shown are two terminal NANOR®-type devices containing active ZrO_2–PdD nanostructured material at their core. Used for this study was an M- NANOR®.

referred to as ZrO_2–PdD. The enclosure is tightly fit with the electrodes. It is a long, expensive, arduous effort to prepare these preloaded nanocomposite CF/LANR devices, whose development has required control of their breakdown states and quenching tendencies. The NANOR® component used for this work is a sixth generation CF/LANR device, smaller than 2 cm length, with less than 50 mg of active LANR material. Although small in size, this is actually not *de minimus* because the LANR excess power density was more than 19,500 W/kg of nanostructured material [11,13].

2.3. Methods – electronic properties of nanomaterials

We previously reported sudden changes of, and generally large, electrical resistances of such NANOR®-type devices containing nanostructured materials [13,15].The proprietary microprocessor controlled system semiquantitatively examines and drives the NANOR, examining it for heat-production activity, linearity, time-invariance, and even the impact of additives and applied fields. The LANR preloaded, stabilized NANORs were driven by a high DC voltage circuit up to 1000^+ V rail voltage. The duty cycle was split with half going to a control portion consisting of a carefully controlled electrical DC pulse into an ohmic resistor which was used to thermally calibrate the calorimeter [13, 17–19]. The NANOR® system used had previously been driven for more than a year with careful evaluation for energy gain under a variety of conditions, including during the January, 2012 IAP MIT Course on CF/LANR, and later during a long term low-power open demonstration at MIT which ran from Jan. 30, 2012 through mid-May 2012 [12,14]. The NANOR®-type preloaded LANR device openly demonstrated clear cut energy gain (COP) which ranged generally from 5–16 (e.g. 14.1 ($\sim$1412%) while the MIT IAP course was ongoing, 11). In order to measure the incremental increase of penetrating ionizing radiation output of an active nanocomposite ZrO_2–PdD LANR material, the NANOR was driven at its well-characterized optimal operating point. The system was previously well characterized over many months at MIT.

2.4. Methods – power and energy considerations

Data acquisition was taken from voltage, current, temperatures at multiple sites of the solution, and outside of the cell, and even as a 4-terminal measurement of the NANOR's internal electrical conductivity [13, 19,16–18,11]. Data acquisition sampling was at data rates of 0.20–1 Hz, with 24+ bit resolution; voltage accuracy $0.015^{\pm 0.005}$ V, temperature accuracy <0.6°C. The noise power of the calorimeter is in the range of $\sim$1–30 mW. The noise power of the Keithley current sources is generally $\sim$10 nW. Input power is defined as $V{\times}I$. There is no thermoneutral correction in denominator. Therefore, the observed power is a lower limit. The instantaneous power gain [power amplification factor (non-dimensional)] is defined as $P_{\text{out}}/P_{\text{in}}$. The energy is calibrated by at least one electrical joule control (ohmic resistor) used frequently, and with time integration for additional validation. The excess energy, when present, is defined as $(P_{\text{output}} - P_{\text{input}}) \times$ time.

The amount of output energy (and therefore, both power, and energy, gain) is determined from the heat released producing a temperature rise, which is then compared to the input energy. Observed signals are determined by parallel diagnostics including thermometry, focused heat flow measurement, and isoperibolic calorimetry, and then semiquantitively repeatedly calibrated by an ohmic (thermal) control located next to the NANOR [10,11,15–17]. The output of the NANOR is compared to the output of the precisely driven ohmic control. The result is heat measurement of this preloaded NANOR®-type LANR three (3) ways ending in calorimetry, input-power-normalized ΔT (dT/P_{in}), and input power normalized heat (HF/P_{in}) [11]. These three methods of verification are pooled to derive very useful information, including the energy produced ("excess energy") and sample activity.

2.5. Methods – ionizing radiation detection

In order to maximize the likelihood of detecting any possible incremental increase of penetrating ionizing radiation output of an active nanocomposite ZrO_2–PdD LANR material, the NANOR® was driven directly next to a vicinal, in situ Geiger–Müller tube, embedded in the calorimeter (Fig. 3a). A second custom DAQ was used. In addition, the tube chosen was a (SI29BG) Russian military tube (also called SI29BG). It is comparatively small and sensitive to both β and γ ionizing radiation. Here, the military standard СИ29БГ Geiger–Müller tube was chosen over the more popular СБМ-20 (SBM-20) tube because of the shorter minimum Dead Time of 95 μs, and four times greater sensitivity. The ÑÈ29ÁÃ has a Gamma Sensitivity to ^{60}Co (cps/mR/h) of 44–52. Therefore, the conversion factor

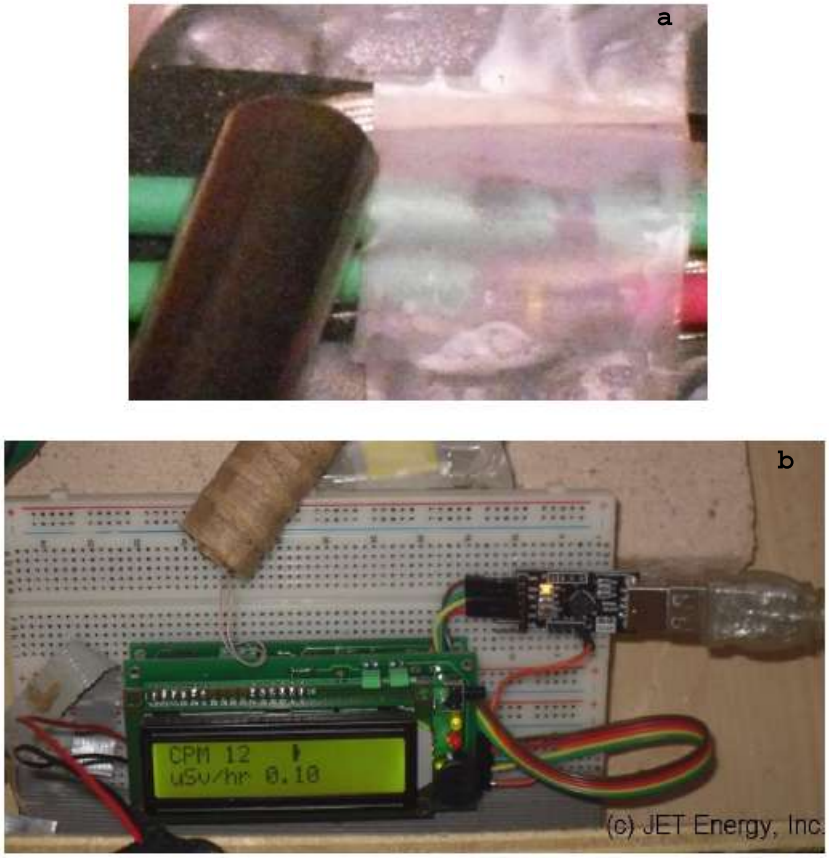

Figure 3. (a) Shown is the central region within the calorimeter. The horizontally directed NANOR-type quantum electronic component, containing active ZrO_2–PdD nanostructured material, is located within the upper green cylinder. The Geiger Müller tube is shifted off of the active site (rectangular appearing black area located just above the ohmic resistor (to the right of its yellow-colored band;, and off to the right from the center) and shown moved about twice its width to the left from its normal location for the photograph. The Geiger–Müller tube is just outside of the tape and to left for the photograph. In addition, the holders, thermal ballasts, thermal conduction materials, vicinal detectors, and electrical insulation, have been removed to more clearly show this. (b) The modified Arduino delivered 500–700 V to the GM tube while also recording GM output, integrating that to CPM, and a 10 min running average of CPM, and converting to microSv/h. The output was delivering (including tube voltage) to the USB to the second DAQ, and to a charlieplexed digital output over the Arduino (shown with background levels).

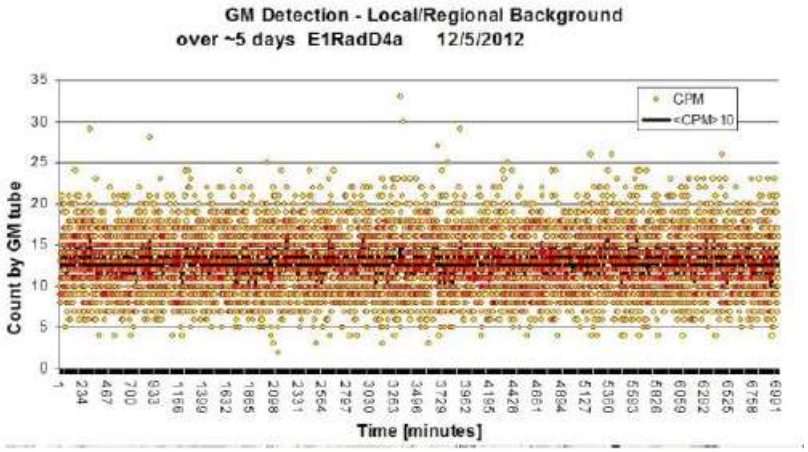

Figure 4. A five-day collection of background data. Shown is the 10 min moving average of the CPM, ⟨CPM⟩10, as a function of time (Fig. 5). For this long measurement, the LANR NANOR, the ohmic control, and the electrical driving system was in place but remained electrically off, for the entire time.

used was 123.147 cpm/μSv/h. A TTL serial converter based on SILABS CP2102 chip was necessary to connect the GM board to PC. The Geiger Müller system was calibrated both for microprocessor function and detection sensitivity.

In order to minimize the impact of environmental contamination, we used very long, autonomously-run, times for the measurements. An ATMEGA328 autonomous system was used to remove interaction with, and contamination from, ^{40}K, because humans are a major cause of incident background radiation. Also used were an Arduino [ATMEGA328 processor] driven/controlled Geiger counter dosimeter, with confirming LCD shield tube (simultaneously displaying the Count Per Minute (CPM) and equivalent dose rate of radiation in μSv/h) and USB connection to a second logging computation system. The Arduino sketch was designed to record to computer via serial port the counter outputs CPM, μSv/h and the voltage across the tube, as data in 1 min intervals. The GM count was taken each minute, and the 10 min moving average of that is designated ⟨CPM⟩10. In order to minimize the likelihood of cross-talk and other sources of error, the Geiger–Müller in situ dosimeter's computer and power connections were separate from the normal DAQ and driving circuits. The Geiger detector and ATMEGA328 required 5.5 and 16 mA, respectively, for a total of 22 mA. Because the verification LCD backlight, when connected pushed the total current required to 41 mA, therefore a separate computer system was used. Recalibration of the calorimetry was performed prior to the experiment in a control, and normal CF/LANR sequence. Thereafter, the NANOR drive system (NANOR® EXPLORERTM) and the vicinal Geiger–Müller tube СИ29БГ(SI29BG) detector operated over months through a series of background, thermal controls, and LANR drive sequences, and LANR components.

3. Results

3.1. Background

First, we measured the background over several weeks. Shown below is 5 days of that control (Figs. 4 and 5). The long-term time-averaged detected background was $12.68^{\pm 3.40}$ nanosieverts/h.

3.2. Derivation of "High Pass Filter"

Then, a high pass filter was used on the counts per minute, especially the 10 min average to maximize detection. An example is in Fig. 5. Examination revealed the following: For example, ⟨CPM⟩10 only went above 16.0 thrice in 5 days, and ⟨CPM⟩10 never went above 16.4. However, during the shorter time that the NANOR was driven, ⟨CPM⟩10 did exceed that level four times, and two of those events were higher than 16.5.

3.3. Incremental increase from CF/LANR

Next, we determined the incremental increase from the CF/LANR device. The long-term time-averaged emission was determined by subtracting the detected background from the observed output when the device was active. This became $13.11^{\pm 3.72} - 12.68^{\pm 3.40}$ with the CF/LANR component in peak active mode. There was a maximum (peak incremental difference observed of ∼2.5 nanosieverts/h. This should be compared with the background irradiation from internal irradiation sources within every person, mainly from internal ^{40}K and uranium and thorium, which contributes ∼46 nanosieverts/h.

3.4. Irregularly irregular emissions

This method of analysis with a high pass filter derived from the running 10 min average of the CPM by a Geiger–Müller tube located vicinal to the self-contained NANOR®-type CF/LANR quantum electronic component, containing active preloaded ZrO_2–PdD nanostructured material at its core was used with isoperibolic calorimetry, calibrated by ohmic controls. Shown in Figs. 1 and 6 are the results, including one which occurred during some additional very low level thorium irradiation. In the figures below, the 10 min average CPM is shown on the right hand y-axis. Three types of regions are shown including background, thermal ohmic heating (labeled "control"), and the active LANR device (labeled "NANOR") which is operated at a variety of electrical input powers, as was the thermal ohmic control. (The 2% thoriated electrodes, discussed below in a separate experiment, were not present here.) For clarity, the periods without any input are not labeled.

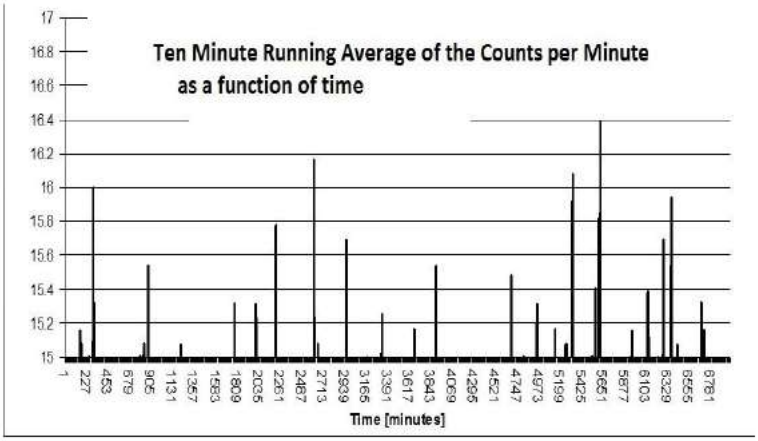

Figure 5. A five-day collection of "high-pass" background data. Shown is ⟨CPM⟩10, as a function of time, but only shown are those events which exceeded ⟨CPM⟩10 greater than 15. In the following, a high pass filter was used which only "passes" the ⟨CPM⟩10 which are greater than ∼15.5.

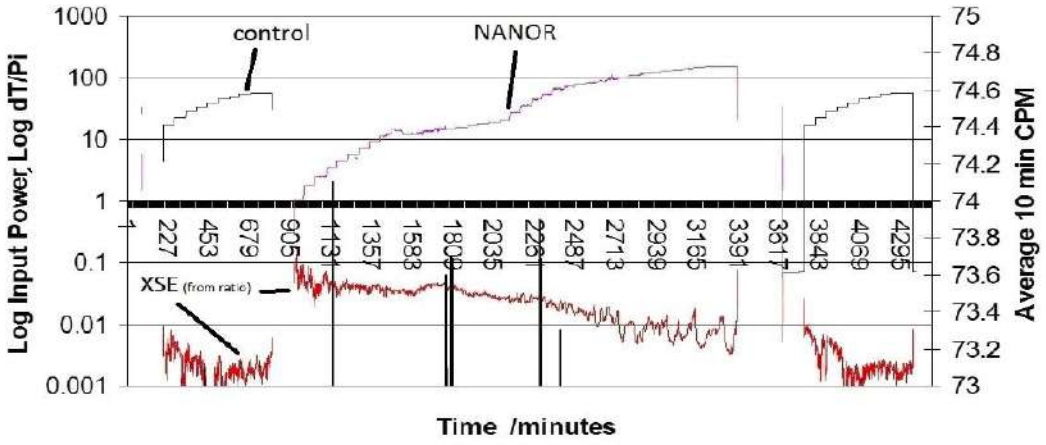

Figure 6. Calorimetry and gamma measurements of background, thermal control and a CF/LANR system. with a 2% Thoriated Rod nearby – Shown are the Input Power in milliwatts, Resulting delta-Temperature rise which is input power normalized [as the logarithm on the left], and the 10 minute average output count by a Geiger Müller tube, which was located vicinal to the self-contained CF/LANR quantum electronic component containing active preloaded ZrO_2–PdD nanostructured material at its core. The activity of the active CF/LANR system is XSE (obtained from the ratio of dT/P_{in} (CF/LANR) to dT/P_{in} (control)).

Attention is directed to the observation of very rare, irregularly spaced, distinguishing emissions were observed with LANR compared to background, and compared to the ohmic thermal control). These are distinguishing emissions of penetrating radiation or other emissions (e.g. gammas) observed with LANR NANORs driven at their OOP compared to background and compared to the ohmic thermal control. These peak bursts are in the range of ∼24.6 nanosieverts/h momentarily during these emissions, which are infrequent and irregularly irregular. Correcting for the irregular and infrequent nature of the emission, this time averages out to become an incremental output of circa ∼0.14 nanosieverts/h for this functioning demonstration NANOR device. Considering the electrical input power, this time averages out to become circa ∼8.5 nanosieverts/h/W incremental output penetrating radiation for this functioning demonstration device very close up to the NANOR without any shielding.

3.5. Impact of additional thorium irradiation

In order to determine if additional irradiation by ionizing irradiation to the NANOR might increase or change the output of the NANOR®-type LANR component (Fig. 2) and as an additional control, a series of long term runs over weeks were also made with several vicinal 2% thoriated tungsten electrodes (*Sylvania*; not connected to any power source). This active NANOR®-related differential even occurred during the thorium irradiation examination.

In an experimental run similar to that shown in Fig. 1, there was for this run, extending over a long time, a continuous background irradiation of the LANR device (during background, control, and its active state) from 2% thoriated-tungsten electrodes which were not electrically connected to anything. This is shown in Fig. 6. Attention is directed to the observation of, again, very rare, irregularly spaced, distinguishing emissions were observed with LANR compared to background, and compared to the ohmic thermal control.".

Additionally, note that there was no increase in excess heat OR incremental penetrating output observed for the LANR system by the additional irradiation from the nearby 2% thoriated electrodes. There was still a NANOR®-related differential in output which persisted during the thorium irradiation, even with the much higher CPM secondary to the additional thorium irradiation (due to the alpha and other decays).

4. Conclusion

4.1. Interpretation

There is an incremental outputs associated with CF/LANR at the active point of the OOP manifold for very brief and irregular times. These are not seen as frequently, if at all, during the control sequences involving background. These results are not from a cosmic ray shower because similar groups of these bursts did not occur during background runs (Fig. 3), nor during thermal controls. These results demonstrate that the incremental output of gamma by this CF/LANR device heralds a nuclear reaction controlled by applied electric field intensities using preloaded deuterides.

Further corroborating that this is a real effect, attention is directed to the fact that when the excess heat disappeared, so did the bursts. Of special note is the fact that the bursts did occur sometimes immediately after the calibration pulse, or the run, of the NANOR.

In conclusion, this is further confirmation that LANR is indeed an important nuclear process. The maximum burst output, during one of the irregularly irregular peaks and very infrequent, is, for this functioning demonstration device, $\sim$ 2.7 μsieverts/h-W. This may be the result of this being an M-NANOR® rather than a conventional NANOR® component since new CF/LANR pathways appear to be available through the second OOP manifold.

In addition, considering the electrical input power, but also correcting for the irregular and infrequent nature of the emission, this time average then becomes circa $\sim$8.5 nanosieverts/h-W incremental output in penetrating radiation emissions for this functioning demonstration device.

Thus, for this system and electrical drive, the emitted radiation is quantitatively measurable, biologically insignificant, and therefore safe. The output should be compared with the background irradiation from people, each of which with their internal ^{40}K and uranium and thorium in their bodies, emits $\sim$ 46 nanosieverts/h. In retrospect, it was fortunate and necessary to have made the equipment autonomous given these findings.

4.2. Future plans

What remains to be determined is the exact nature of the source of the incremental counts and its energy spectrum. These peaks are most likely gamma emission because GM tubes are relatively insensitive to neutrons, however, the GM walls and nearby materials could be a source of additional collision-created ions capable of registering a pulse from neutrons (A. Meulenberg). Some amount of consideration of occupancy, shielding, etc. should now be considered for any very high power CF/LANR device.

5. Acknowledgements

The author is especially grateful to Gayle Verner and Jeffrey Tolleson for their meticulous help in the manuscript and in several idea developments, and to Alex Frank, Peter Hagelstein, Brian Ahern, Jeff Driscoll, Larry Forsley, Pamela Mosier-Boss, Frank Gordon, David Nagel, Robert Smith, Allen Swartz, Charles Entenmann, Val Zavarzin, Ron Kita, Andrew Meulenberg, Ed Pell, and JET Energy and New Energy Foundation for support. NANOR® and PHUSOR® are registered trademarks of JET Energy, Incorporated. NANOR®-technology, and PHUSOR®-technology, and other discussed IP herein, are protected by U.S. Patents D596724, D413659 and several other patents pending.

Bibliography

[1] Swartz, Mitchell R., Survey of the observed excess energy and emissions in lattice assisted nuclear reactions, *J. Scientific Exploration* **23**(4) (2009) 419–436.

[2] Swartz, Mitchell R., P. Hagelstein et al., Amplification and restoration of energy gain using fractionated magnetic fields on ZrO_2–PdD nanostructured CF/LANR quantum electronic component, *Proc. ICCF-18*, Missouri, USA, 2013.

[3] Swartz, Mitchell R., Phusons in nuclear reactions in solids, *Fusion Technol.* **31** (1997) 228–236.
[4] Swartz, Mitchell R. and G. Verner, Bremsstrahlung in hot and cold fusion, *J. New Energy* **3**(4) (1999) 90–101.
[5] Iyengar, P.K. and M. Srinivasan, Overview of BARC studies in cold fusion. in the first annual conference on cold fusion, University of Utah Research Park, Salt Lake City, Utah, National Cold Fusion Institute, 1990.
[6] Miles, M. et al., Correlation of excess power and helium production during D_2O and H_2O electrolysis using palladium cathodes, *J. Electroanal. Chem.* **346** (1993) 99–117.
[7] Srinivasan, M. et al., Observation of tritium in gas/plasma loaded titanium samples. in anomalous nuclear effects in deuterium/solid systems, *AIP Conferencpe Proceedings 228*, American Institute of Physics, New York, 1990.
[8] Li, X.Z. et al., The precursor of cold fusion phenomenon in deuterium/solid systems. in anomalous nuclear effects in deuterium/solid systems, *In AIP Conference Proceedings 228*, American Institute of Physics, New York, 1990.
[9] Mosier-Boss, P.A., Szpak, S., Gordon, F.E. and Forsley, L.P.G., Use of CR-39 in Pd/D co-deposition experiments, *Eur. Phys. J.–Appl. Phys.* **40** (2007) 293–303.
[10] Swartz, Mitchell R., G. Verner and A. Weinberg, Non-thermal near-IR emission from high impedance and codeposition LANR devices, *Proc. ICCF-14*, D.J. Nagel and M. Melich (Eds.), Washington DC, USA, ISBN: 978-0-578-06694-3, 343, (2010).
[11] Swartz, Mitchell R., Consistency of the biphasic nature of excess enthalpy in solid state anomalous phenomena with the quasi-1-dimensional model of isotope loading into a material, *Fusion Technol.* **31** (1997) 63–74.
[12] Swartz, Mitchell R., Optimal operating point manifolds in active, loaded palladium linked to threedistinct physical regions, *Proc. ICCF-14*, D.J. Nagel and M. Melich (Eds.), Washington DC, USA, ISBN: 978-0-578-06694-3, 639, (2010).
[13] Swartz, Mitchell R., G. Verner and J. Tolleson, Energy gain from preloaded ZrO2–PdNi–D nanostructured CF/LANR quantum electronic components, *Proc. ICCF-17,* 2012.
[14] Swartz, Mitchell R. and P.L. Hagelstein, Demonstration of energy gain from a preloaded ZrO_2–PdD nanostructured CF/LANR quantum electronic device at MIT, *Proc. ICCF-17,* Daejeon, Korea, 2012.
[15] Swartz, Mitchell R., LANR nanostructures and metamaterials driven at their optimal operating point, *J. Condensed Matter Nucl. Sci.* **6** (2012) 149.
[16] Arata, Y. and Zhang, Y.C., Anomalous production of gaseous ^{4}He at the inside of DS-cathode during D_2-electrolysis, *Proc. of the Japan Academy Series B*, 75, 281; Arata, Y. an Zhang, Y.C. (1999). Observation of anomalous heat release and helium-4 production from highly deuterated fine particles, *Jpn. J. Appl. Phys.* **38**(2) (199) L774; Arata, Y. an Zhang, Y., The establishment of solid nuclear fusion reactor, *J. High Temp. Soc.* **34**(2) (2008) 85.
[17] Swartz, Mitchell R., Can a Pd/D_2O/Pt device be made portable to demonstrate the optimal operating point?, *Condensed Matter Nuclear Science, Proc. ICCF-10*, P.L. Hagelstein and S.R. Chubb (Eds.), Cambridge, MA, USA, World Scientific, NJ, ISBN 981-256-564-6, 29-44; 45-54 (2006).
[18] Swartz, Mitchell R., Excess power gain using high impedance and codepositional LANR devices monitored by calorimetry, heat flow, and paired stirling engines, *Proc. ICCF-14*, D.J. Nagel and M. Melich (Eds.), Washington DC, USA, ISBN: 978-0-578-06694-3, 123, (2010).
[19] Swartz, Mitchell R. and G. Verner, Excess heat from low electrical conductivity heavy water spiral-wound Pd/D_2O/Pt and Pd/D_2O–$PdCl_2$/Pt devices, *Condensed Matter Nuclear Science, Proc. of ICCF-10*, Peter L. Hagelstein and Scott S.R. Chubb (Eds.), Cambridge, MA, USA, World Scientific, NJ, ISBN 981-256-564-6, 29-44; 45-54 (2006).